



Characterization of CO₂ Laser Photoacoustic Spectrometer Intracavity Configuration and Its Application in Measuring Acetone Gas in Human Breath

Mitrayana^{1*}, Nurul Muyasarah¹, Mohammad Ali Joko Wasono¹,
and Mohammad Robikhul Ikhwan²

¹Physics Department, Faculty of Mathematics and Natural Science, Universitas Gadjah Mada,
Sekip Utara, Bulaksumur, Yogyakarta 55281, Indonesia

²Internal Medicine Ward, RSUP Dr. Sardjito, Faculty of Medicine, Universitas Gadjah Mada,
Jalan Kesehatan, Kabupaten Sleman, Yogyakarta 55281, Indonesia

Abstract: Photoacoustic spectrometer is a very effective instrument for detecting low concentration gasses. In this research, a CO₂ laser photoacoustic spectrometer intracavity configuration was characterized and applied for measuring acetone gas concentration in human exhaled breath during exercise on a treadmill. The characterization included laser power optimization, scanning laser spectrum, making resonant curve and quality factor, measuring noise and background signal, determining lowest detection and linearity curve. Acetone gas concentration was determined by analyzing normalized photoacoustic signal using multicomponent matrix. The optimum power was obtained at 32.4 ± 0.5 W and CO₂ laser spectrum consisted of four line groups. The highest laser absorption line of standard acetone gas was determined at 10P20. Quality factor was obtained at 14.6 ± 0.6 , noise at $1.7 \pm 0.2 \mu\text{V}/\text{Hz}^{1/2}$, background signal at 10P20 0.001 to 0.004 mV, lowest detection limit of acetone gas at $110 \pm 14 \text{ ppbV}$, and acetone gas linearity gradient on 10P20 was at $k_{22} = 0.0140 \pm 0.0007$. Acetone gas concentration in human exhaled breath after exercising on treadmill decreased from 43 % to 79 % than before.

Keywords: Acetone gas concentration, exercise, intracavity configuration CO₂ laser photoacoustic spectrometer, treadmill

1. INTRODUCTION

Photoacoustic spectrometer (PAS) is a very effective instrument for detecting trace gasses at low concentrations. For the detection of sample gas, PAS is based on energy resonance between radiation source and excitation energy of gaseous molecule. Photoacoustic spectrometer had been applied in all research fields [1–4]. Schramm et al. [1] succeeded in detection of the NO₂, N₂O, and SO₂ gases from diesel machines exhaust by using PAS. Schilt et al. [2] also used PAS to monitor the ammonia amount in the semiconductor industrial area. Huber et al. [3] succeeded in developing the CO₂-Sensor for Automotive Applications by following the photoacoustic principle. Popa and Petrus [4] used CO₂ laser PAS to investigate the effect of heavy metals on plants by detecting the emitted ethylene and ammonia gas.

A sample is placed at photoacoustic cell, radiated by laser radiation of which the intensity is modulated on photoacoustic cell resonance frequency. The gaseous molecule absorbs laser radiation energy and it is excited to a higher state. The excited state loses its energy by collisions. The collisions between molecules cause the increasing kinetic energy, and then it causes the increase in temperature. And the increase in temperature causes the increase in pressure. Because the intensity of laser radiation is

modulated, the pressure fluctuates. The fluctuation of pressure causes the acoustics which can be detected using microphone [5].

In this research, a CO₂ laser photoacoustic spectrometer intracavity configuration had been characterized and applied for measuring acetone gas concentration of human exhaled breath during exercise on treadmill. CO₂ laser is radiation source which radiates infrared beam at the wavelength area of 9.2 μm to 10.8 μm where there is more than 250 molecular gasses of environmental concern with atmospheric, medical and scientific spheres exhibiting strong absorption bands [6].

Acetone gas is a diabetes mellitus biomarker [7, 8]. Patients' pancreas with diabetes mellitus can not produce quite insulin to absorb glucose produced by food, whereas high blood glucose level causes the formation of acetone gas [9]. Diabetes mellitus can be diminished by exercises such as walking on the treadmill [10].

2. MATERIALS AND METHODS

The photoacoustic spectrometer characterizations include laser power optimization, scanning laser spectrum, making resonant curve and quality factor, measuring noise and background signal, determining lowest detection and linearity curve (Fig. 1).

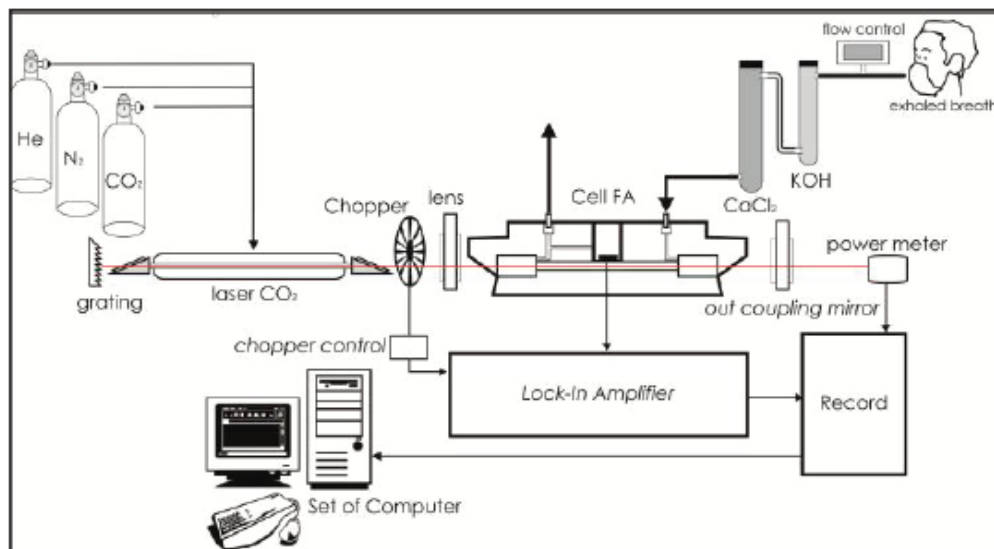


Fig. 1. The CO₂ laser photoacoustic spectrometer intracavity configuration scheme.

Measuring of acetone gas concentration of human exhaled breath during exercise on treadmill began by taking the volunteer breath and saving it in a sample bag through KOH and CaCl₂ scrubber. A scrubber was used as the CO₂ and H₂O absorber. Volunteer breath was taken five times, before exercise (decision to- 1), after warming up (decision to- 2), after conditioning (decision to- 3), after cooling down (decision to- 4) and 5 min after exercise (decision to- 5) (see Fig. 8 and Fig. 9).

- Warming up: walking on the treadmill 1.2 km h⁻¹ for 5 min.
- Conditioning: walking on the treadmill 2.4 km h⁻¹ for 20 min.
- Cooling down: walking on the treadmill 1.2 km h⁻¹ for 5 min.

Volunteer breath was flowed into a photoacoustic spectrometer for detecting and producing photoacoustic signal. Since the photoacoustic signal is proportional to laser power, it must be normalized.

The normalized photoacoustic signal is a fluctuating time function needed to choose the constant average region. Acetone gas concentration was determined by analyzing normalized photoacoustic signal using a multicomponent matrix as shown in Equation (1).

$$(S_n)_i = \sum_{j=1}^3 k_{ij} C_j, (i = 1, 2, 3) \quad (1)$$

where C_j is gas concentration, $(S_n)_i$ is normalized photoacoustic signal at highest absorbtion laser line, k_{ij} is a calibration factor.

Acetone gas concentration after (C_i) and before (C_o) exercising on the treadmill was compared using Equation (2).

$$\Delta C = \frac{C_0 - C_i}{C_0} \times 100 \% \quad (2)$$

where ΔC is the acetone gas concentration difference. The acetone gas concentration of human breath with and without excercises on the treadmill was compared.

3. RESULTS AND DISCUSSION

3.1. The Characterization of CO₂ Laser Photoacoustic Spectrometer Intracavity Configuration

In this research, CO₂ laser was operated at 8.32 kV to 9.04 kV and 11.93 mA to 12.84 mA, because at this voltage and this current, laser can produce lasing easily. The optimum power was obtained at (32.4 ± 0.5) W and CO₂ laser spectrum consisted of four line groups, as shown in Fig. 2.

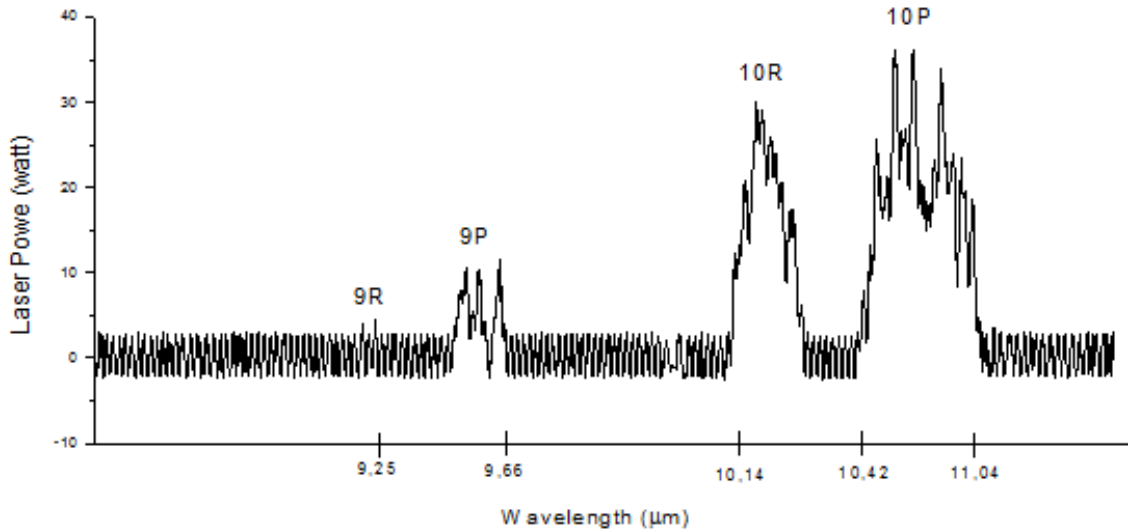


Fig. 2. CO₂ laser spectrum.

The optimum power can be obtained by optics aligning. Grating, laser tube, chopper, photoacoustic cell and outcoupling mirror was aligned. He, N₂ and CO₂ flow scale were arranged at 30, 70 and 50. Optic component must be cleaned to obtain the optimum power because the dust on optic component surface can interfere laser propagation.

Photoacoustic cell was designed as resonator to amplify the photoacoustic signal. Resonance curve of acetone gas is shown in Fig. 3. The resonance frequency was obtained at $f_{\text{res}} = (1650 \pm 5)$ Hz and the bandwidth, at $f_{\text{res}} = (113 \pm 5)$ Hz. Chopper was arranged at this frequency, so that laser radiation can be

resonated with the sample in photoacoustic cell. Quality factor (Q) can be obtained using Equation (3). Quality factor was obtained at 14.6 ± 0.6 .

$$Q = \frac{f_{res}}{\Delta f} \quad (3)$$

where Δf is resonance curve bandwidth when the signal is the $1/\sqrt{2} \times$ maximum signal.

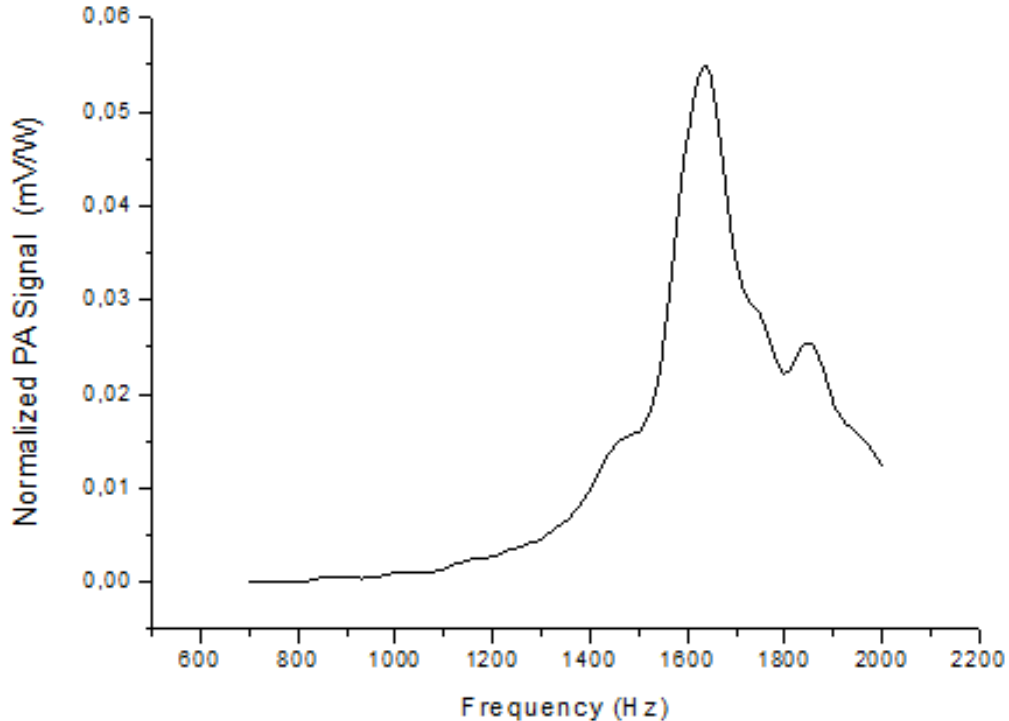


Fig. 3. Resonance curve of acetone gas.

The highest laser absorption line of standard acetone gas, standard ethylene gas, standard ammonia gas were known using the absorption spectrum of each gas. Every gas absorbs a laser line or more and resonates at a specific laser line. Absorption spectrum of acetone gas is shown in Fig. 4. The highest laser absorption line of the standard acetone gas was determined at 10P20.

Signals which interfere photoacoustic signal are noise and background signals. The noise is caused by acoustical and electrical vibrations. The noise was obtained at $1.7 \pm 0.2 \mu\text{V}/\text{Hz}^{1/2}$. It is used to determine the lowest detection limit. The noise of photoacoustic spectrometer is shown in Fig. 5.

The background signal was measured before measuring the photoacoustic signal. The example of the background signal measured at the laser line 10P20 is shown in Fig. 6. The background signal at 10P20 was 0.001 mV to 0.004 mV.

System sensitiveness of photoacoustic spectroscopy is determined by the lowest detection limit given by:

$$BDT = \frac{C}{(S_n / N)} \quad (4)$$

where C is acetone gas concentration, S_n is normalized photoacoustic signal, and N is noise. The lowest detection limit of acetone gas was $110 \pm 14 \text{ ppbV}$.

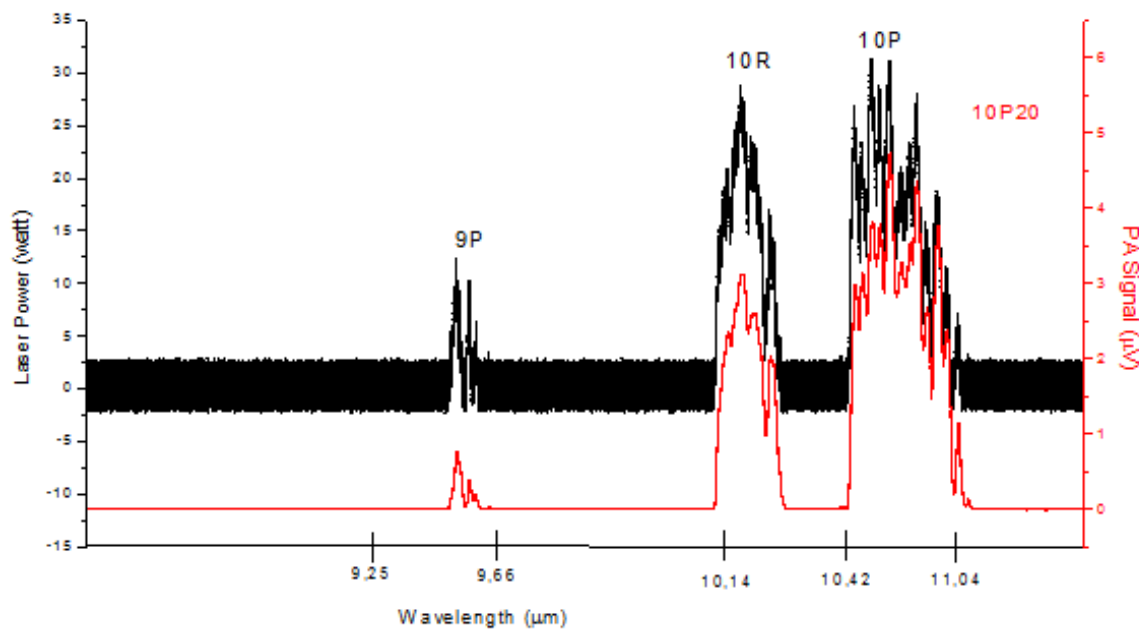


Fig. 4. Absorption spectrum of acetone gas.

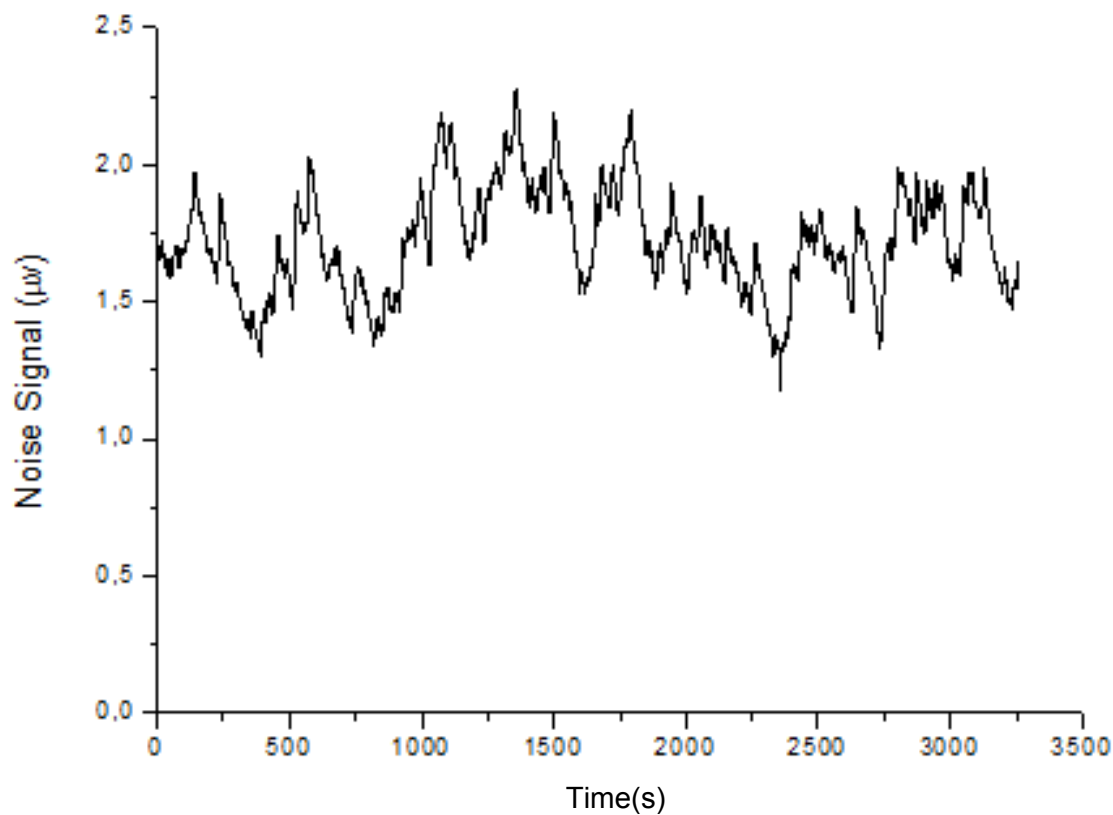


Fig. 5. Noise of photoacoustic spectrometer.

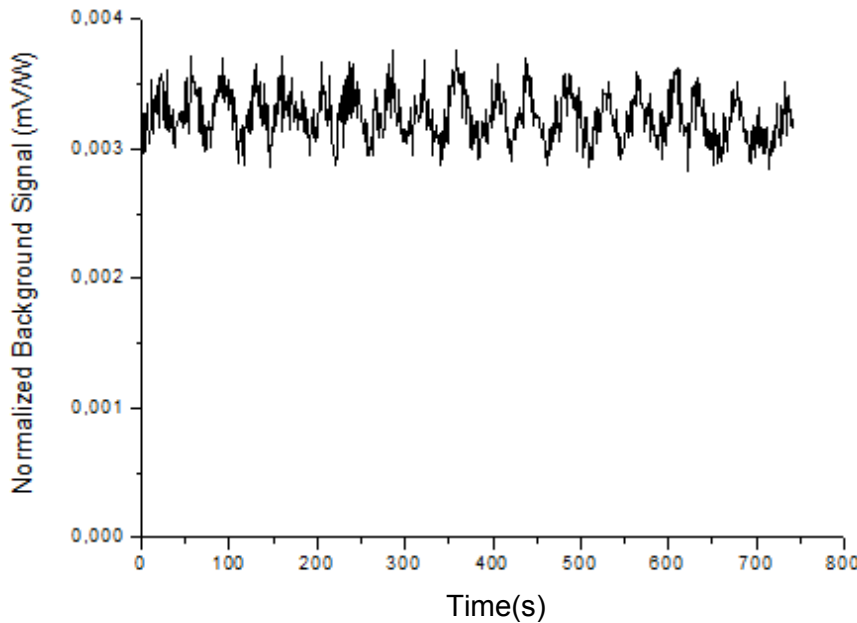


Fig. 6. Background signal.

The correlation between gas concentration and photoacoustic signal is determined by the calibration factor using multicomponent analysis, an analysis of sample that consists of more than one gases. Gases used in this research are ethylene, acetone and ammonia. Analysis was done by measuring the photoacoustic signal of each gas at each laser line where the highest absorption occurred. It is shown in gas absorption spectrum that the highest absorption line of acetone gas was determined at 10P20, ethylene gas at 10P14, and ammonia gas at 10R14. Every gas was broken up into some concentrations. The correlation between the gas concentration and the photoacoustic signal was drawn as a linearity curve.

Linearity curve of acetone gas at laser line 10P20 is shown in Fig. 7. The acetone gas linearity gradient was $k_{22} = 0.0140 \pm 0.0007$. The correlation factor of this linearity was $R^2 = 0.98807$. Gradient is a calibration factor, the correlation between gas concentration and photoacoustic signal. The gradient of each linearity curve is used as a matrix component of the multicomponent analysis as shown in Equation (5).

$$\begin{pmatrix} (S_n)_1 \\ (S_n)_2 \\ (S_n)_3 \end{pmatrix} = \begin{pmatrix} 0.029 & 0.00115 & 0.00110 \\ 0.012 & 0.0140 & 0.0120 \\ 0.00051 & 0.00019 & 0.025 \end{pmatrix} \begin{pmatrix} C_1 \\ C_2 \\ C_4 \end{pmatrix} \quad (5)$$

Gas concentration was determined by matrix inverse given by:

$$\begin{pmatrix} C_1 \\ C_2 \\ C_3 \end{pmatrix} = \begin{pmatrix} 35.010339 & -2.7477681 & -0.2130922 \\ -29.351669 & 74.235621 & -35.059278 \\ -0.4710460 & -0.5454753 & 40.774024 \end{pmatrix} \begin{pmatrix} (S_n)_1 \\ (S_n)_2 \\ (S_n)_3 \end{pmatrix} \quad (6)$$

Hence, ethylene, acetone and ammonia gas concentration become:

$$\begin{aligned} C_1 &= 35.010339(S_n)_1 - 2.7477681(S_n)_2 - 0.2130922(S_n)_3 \\ C_2 &= -29.351669(S_n)_1 + 74.235621(S_n)_2 - 35.059278(S_n)_3 \\ C_3 &= -0.4710460(S_n)_1 - 0.5454753(S_n)_2 + 40.774024(S_n)_3 \end{aligned} \quad (7)$$

where C_1 , C_2 dan C_3 respectively are ethylene, acetone and ammonia gas concentrations. $(S_n)_1$, $(S_n)_2$ and $(S_n)_3$ respectively are normalized photoacoustic signals at laser lines 10P14, 10P20 and 10R14.

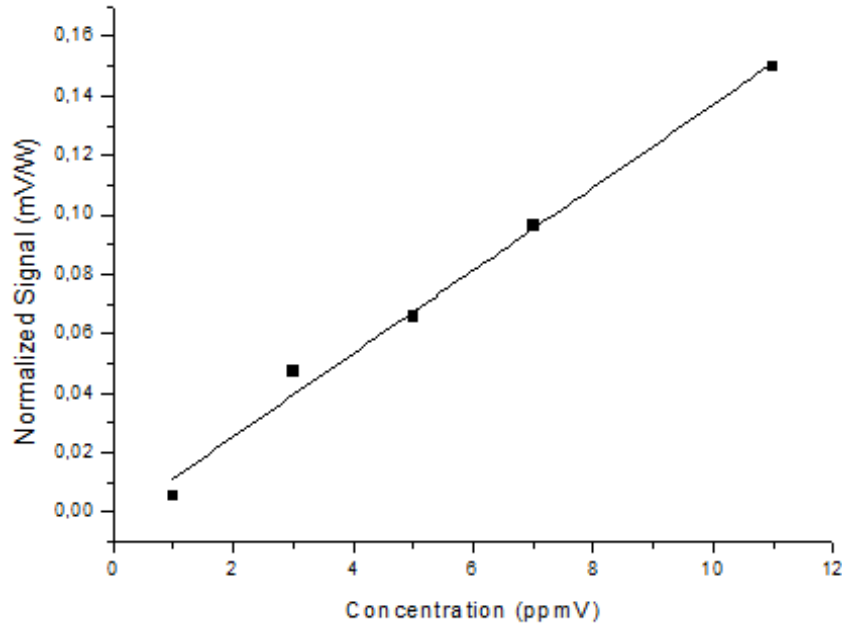


Fig. 7. Linearity curve of acetone gas at laser line 10P20.

3.2. Measuring Acetone Gas Concentration of Human Breath During Exercise on a Treadmill

An acetone gas concentration graph of human exhaled breath during exercise on treadmill is shown in Fig. 8.

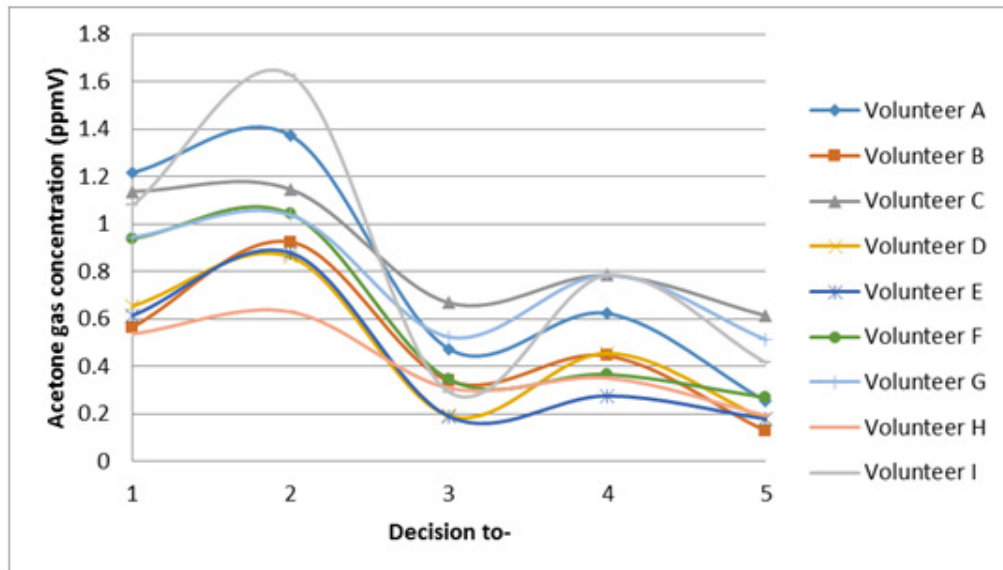


Fig. 8. Acetone gas concentration graph of human exhaled breath during exercise on a treadmill.

The acetone gas concentration graph of human exhaled breath during exercise on treadmill is compared with the acetone gas concentration graph of human exhaled breath without any activity as shown in Fig. 9.

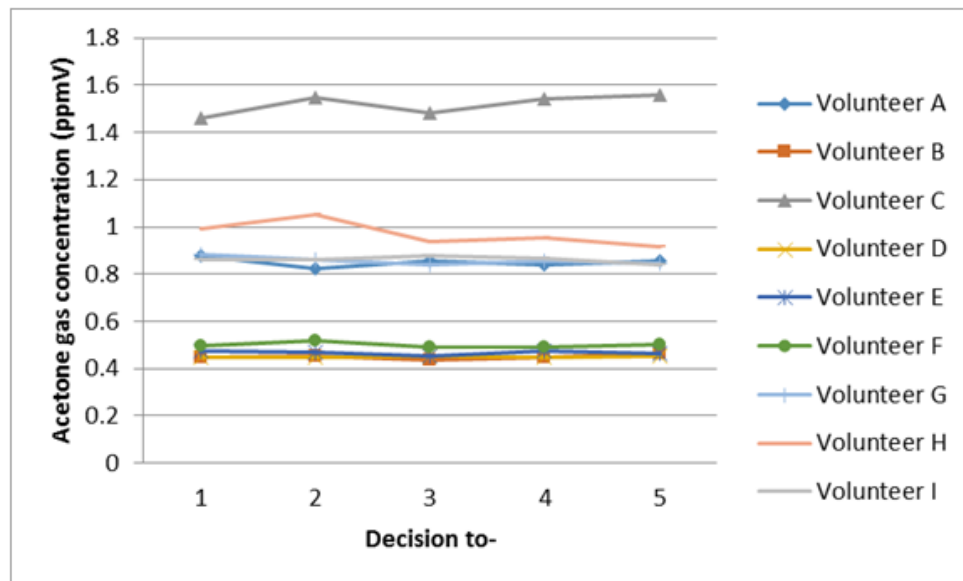


Fig. 9. Acetone gas concentration in exhaled breath of humans doing no activity.

Acetone gas concentration of human exhaled breath during exercise on treadmill is more fluctuative than that without any activity because the acetone gas concentration is interfered by the blood glucose level. The blood glucose level can be interfered by exercises. As shown in Fig. 8, after warming up, the acetone gas concentration is higher than before exercises. Warming up was done 5 min, exercising less than 20 min causes the liver to release the blood glucose that is saved as fuel. The increase in the acetone gas concentration is supposed to be caused by the blood glucose released, so it indicates a high signal when being detected. After conditioning, the acetone gas concentration drastically decreases, it is lower than the concentration before exercises. Conditioning was done for 20 min, exercising 20 min, or if it is more than 20 min it may cause the muscles to take the blood glucose for fuel and it decreases the blood glucose totality [5]. After cooling down, the acetone gas concentration increases again, causing the liver to release the blood glucose again. Amount 5 min after exercises, the acetone gas concentration is lower than that before exercises. The acetone gas concentration of human exhaled breath after exercising on treadmill decreased at 43 % to 79 % than before. It is in line with the hypothesis that acetone gas concentration of human exhaled breath after exercising on treadmill decreases than before because exercises can reduce the blood glucose level.

4. CONCLUSIONS

The lowest detection limit for acetone gas from the built photoacoustic spectrometer was 110 ± 14 ppbV. The system detected acetone gas from the volunteer breath during exercise on a treadmill using laser CO₂ photoacoustic spectrometer. The acetone gas concentration in human exhaled breath after exercising on a treadmill decreased from 43 % to 79 % compared with concentration in the prior to exercise breath.

5. REFERENCES

1. Schramm D.U., M.S. Sthel, M.G. Silva, L.O. Carneiro, A.J.S.A. Junior & H.Vargas. Application of laser photoacoustic spectroscopy for the analysis of gas samples emitted by diesel engines. *Infrared Physics and Technology* 44:263–269 (2002).
2. Schilt, S., L. Thévenaz, M. Niklés, L. Emmenegger & C. Hüglin. Ammonia monitoring at trace level using photoacoustic spectroscopy in industrial and environmental applications. *Spectrochimica Acta. Part A* 60:3259–3268 (2003).

3. Huber, J., C. Weber, A. Eberhardt & J. Wöllensteiner. Photoacoustic CO₂-sensor for automotive applications. In: *Proceedings of the 30th Anniversary Eurosensors Conference – Eurosensors 2016*. Bársony, I., Z. Zsolt & B. Gábor (Ed.). *Procedia Engineering* 168: 3–6 (2016).
4. Popa, C. & P. Mioara. Heavy metals impact at plants using photoacoustic spectroscopy technology with tunable CO₂ laser in the quantification of gaseous molecules. *Microchemical Journal* 134: 390–399 (2017).
5. Harren, F.J.M., G. Cotti, J. Oomens & S.L. Hekkert. Photoacoustic spectroscopy in trace gas monitoring. In: *Encyclopedia of Analytical Chemistry*. Meyer, R.A. (Ed.), John Wiley and Sons, Chichester, p. 2203–2226 (2000).
6. Ivascu, I.R., C.E. Matei, M. Patachia, A.M. Bratu & D.C. Dumitras. CO₂ laser photoacoustic measurements of ethanol absorption coefficients within infrared region of 9.2–10.8 μm. *Spectrochimica Acta. Part A: Molecular and Biomolecular Spectroscopy* 163: 115–119 (2016).
7. Wang, C. & P. Sahay. Breath analysis using laser spectroscopic techniques: Breath biomarkers, spectral fingerprints, and detection limits. *Sensors* 9(10): 8230–8262 (2009).
8. Miekisch, W. & J.K. Schubert. From highly sophisticated analytical techniques to life-saving diagnostics: Technical developments in breath analysis. *Trends in Analytical Chemistry* 25(7): 665–673 (2006).
9. Nayak, S. Influence of aerobic treadmill exercise on blood glucose homeostasis in noninsulin dependent diabetes mellitus patients. *Indian Journal of Clinical Biochemistry* 20(1): 47–51 (2005).
10. Goldoni, M., M. Corradi, P. Mozzoni, G. Folesani, R. Alinovi, S. Pinelli, et al. Concentration of exhaled breath condensate biomarkers after fractionated collection based on exhaled CO₂ signal. *Journal of Breath Research* 7(1): 017101 (2013).